JOURNAL OF COMPUTATIONAL PHYSICS 77, 485–500 (1988)

A Harmonic Expansion for the Magnetic Field of the Helical Solenoid

R. L. DEWAR AND H. J. GARDNER*

Department of Theoretical Physics, Reasearch School of Physical Sciences, The Australian National University, Canberra, A. C. T. 2601, Australia

Received April 3, 1987; revised September 16, 1987

We discuss the boundary value problem for calculating the scalar magnetic potentials inside and outside of a helically symmetric solenoid. Under some circumstances the potentials can be expanded in infinite series of cylindrical harmonics. For a circular cross-section solenoid, we derive a Green's function integral representation of the series coefficients and calculate the radii of convergence of the series by a saddle point method. In some cases the "cylinders of convergence" can intersect the coil, so that there are physically accessible regions where the series fail to converge. Numerical evidence is presented to show that, even in some of these cases, the potentials can be accurately approximated by finite sums of cylindrical harmonics using boundary collocation.

1. INTRODUCTION

The problem of calculating the magnetic field due to a helically symmetric solenoid arises in the treatment of certain stellarator configurations in their large aspect ratio limit. In particular, the helically symmetric limit of the heliac consists of an "$l = 1$" helical solenoid wound about a central axis near which are one or more helical line currrents [1–3]. Helically symmetric geometries are commonly described by a helical coordinate system formed by the linear combination of the conventional cylindrical coordinates (r, ϕ, z) [4]. It is also commonly assumed that helical-solenoidal fields can be well represented by a truncated series of cylindrical harmonics [5]. Such a representation can be desirable for the numerical solution of, for example, the free boundary equilibrium problem which may require the frequent evaluation of the values, and gradients, of the magnetic scalar potential (or the helical flux) on an iterated coordinate grid [6, 7]. (The alternative scheme of evaluating a Biot–Savart-type integral over the solenoidal surface and then using interpolation on a fixed coordinate grid is not only more time consuming but is comparatively wasteful in terms of storage space and involves unnecessary interpolation errors.)

* Present address: Max-Planck-Institut für Plasmaphysik, IPP-EURATOM Association, D-8046 Garching bei München, Federal Republic of Germany.

0021-9991/88 $3.00

Brazier-Smith [8] has noted that the solution of boundary-value problems in potential theory cannot be guaranteed to have a convergent representation as a series of (spherical) harmonic functions in cases where the boundary is not a (spherical) coordinate surface. The central problem of this paper, the calculation of the interior and exterior scalar magnetic potential of a helical solenoid of circular cross section carrying a homogeneous surface current $\mathbf{i}$ (such that $\mathbf{i}\cdot\mathbf{e}_z=0$), provides an illustration of this phenomenon in cylindrical geometry.

Consider the helical solenoid, γ, similar to that shown in Fig. 1. In a helically symmetric configuration, all scalar physical quantities are functions only of r and $\zeta = l\phi - hz$, where (r, ϕ, z) are the usual cylindrical coordinates and the constants l and h give the periodicities in the ϕ and z directions [4]. We shall restrict ourselves to $l=1$ geometries, noting that the transformation to $l>1$ can be effected by rescaling h. The "symmetry vector"

$$\mathbf{u} = \frac{\mathbf{e}_z + hr\mathbf{e}_\phi}{1+h^2r^2} \tag{1}$$

is tangential to γ. We denote the unit outward normal by $\mathbf{e}_n$ and the surface current per unit length by $\mathbf{i}$. Any combination of helically symmetric currents on γ will produce a constant net magnetic circulation, which we shall write as $\mu_0 i_0$, in region B of Fig. 1 and a constant azimuthal circulation, denoted by $\mu_0 I$, in region A.

From Ampère's law, the scalar magnetic potential Φ (such that $\mathbf{B}=\nabla\Phi$) may be written as

$$\Phi^e = \frac{\mu_0 I}{2\pi}\phi + V \qquad \text{in } A \tag{2}$$

and

$$\Phi^i = \mu_0 i_0 z + U \qquad \text{in } B. \tag{3}$$

Here U and V are single-valued, harmonic potentials satisfying

$$\begin{aligned} \nabla^2 V &= 0 \qquad \text{in } A, \\ \nabla^2 U &= 0 \qquad \text{in } B, \\ \mathbf{e}_n\cdot\nabla(V-U) \equiv \partial_n(V-U) &= \partial_n\left(\mu_0 i_0 z - \frac{\mu_0 I}{2\pi}\phi\right) \qquad \text{on } \gamma, \end{aligned} \tag{4}$$

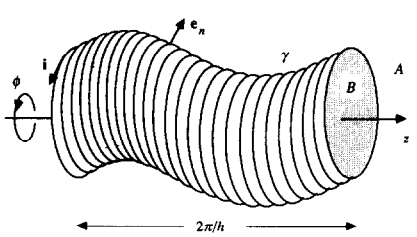

FIG. 1. One period of a helically symmetric solenoid, γ, with the cylindrical coordinate system. The solenoid carries a surface current $\mathbf{i}$ and divides space into an exterior region A and an interior region B.

and

$$V - U = f \qquad \text{on } \gamma,$$

where f can be calculated, to within a constant, from the jump in the longitudinal components of $\mathbf{B}$:

$$\mathbf{e}_n \times (\mathbf{B}^e - \mathbf{B}^i)|_\gamma = \mu_0 \mathbf{i}. \tag{5}$$

It can be shown, from well-known theorems of potential theory, that the three-dimensional boundary value problem of Eq. (4), where U and V have continuous second derivatives and V is bounded at infinity, has a unique solution (to within a constant) [9].

The structure of the rest of this paper is as follows: The conventional Fourier–Bessel series for the interior and exterior potentials are introduced in Section 2. Ignoring the question of convergence for the moment, we then use partial sums of these series to approximate the potentials numerically. The results of three collocation methods for finding the series coefficients are presented in Section 3. The rest of the paper deals with the convergence of the Fourier–Bessel series. A Green's function integral representation for the series coefficients is derived in Section 4. In Section 5 the asymptotic behavior of these coefficients is calculated by the technique of saddle point integration in the complex plane. We derive two transcendental equations whose solutions are the radii of convergence of the series for the interior and exterior potentials. In the discussion of Section 6 we return to the interpretation of the results of Section 3. It appears that the expansion sets may be of some practical use even *outside* of (but close to) their regions of convergence.

2. Choice of the Expansion Set

A Fourier–Bessel expansion for a harmonic potential which is regular at the z-axis but not as $r \to \infty$ is [10]:

$$U = \sum_{n=-\infty}^{\infty} \int_{-\infty}^{\infty} A_n^i(k) \exp(in\phi) \exp(ikz)\, I_n(|k|r)\, dk, \tag{6}$$

where $I_n(|k|r)$ is the modified Bessel function of the first kind of order n. For helically symmetric potentials (such that $\partial_z U|_{r,\zeta} = 0$) which are antisymmetric about the helical ribbon $\zeta = 0, \pi$, so that the current distribution and the magnetic surfaces have reflection symmetry, Eq. (6) becomes

$$U = \sum_{n=1}^{\infty} a_n^i I_n(nhr) \sin(n\zeta). \tag{7}$$

Similarly, an expansion for V which is bounded at infinity but not at $r=0$ is

$$V=\sum_{n=1}^{\infty} a_n^e K_n(nhr)\sin(n\zeta), \tag{8}$$

where the K_n are the modified Bessel functions of the second kind. We shall take the Nth partial sums of these series, U^N and V^N, to be trial solutions of Eq. (4).

THEOREM. *The error functions* $\xi_U = U - U^N$ *and* $\xi_V = V - V^N$ *which satisfy*

$$\begin{aligned} \nabla^2\xi_V &= 0 \qquad \text{in } A,\\ \nabla^2\xi_U &= 0 \qquad \text{in } B,\\ \partial_n(\xi_V-\xi_U) &= \xi_1 \qquad \text{on } \gamma,\\ \xi_V-\xi_U &= \xi_2 \qquad \text{on } \gamma, \end{aligned}$$

take their extremal values on the helical solenoid.

Proof. We assume that γ includes the z-axis. The value of any regular 3D harmonic potential at an interior point must be the arithmetic mean of its values on any sphere which is centred at that point [11]. However, a helically symmetric potential is constant on helical lines (of constant ζ) implying that its value at an interior maximum must be greater than that on all of the neighbouring helical lines. This proves the theorem for ξ_U. The proof for ξ_V is complicated by the point at infinity, but may be accomplished by inverting the exterior region with respect to a cylinder centred on the z-axis and applying the "minimax" principle for second order uniformly elliptic operators [12]. ∎

An obvious corollary is that U, U^N, V, and V^N also take their extremal values on γ.

3. The Collocation Method

Consider a helical solenoid which includes the z-axis and is symmetric about the helical ribbon $\zeta=0,\ \pi$. Suppose that the current is confined to planes of constant z, so that $I=0$ and there is no secular term in region A, and that the distance, $dl=\sqrt{[r^2(d\phi)^2+(dr)^2]}$, along the contour may be parametrized by a variable χ. The unit tangent vector in a constant z plane is

$$\begin{aligned} &(dl)\,\mathbf{e}_t = r(d\phi)\,\mathbf{e}_\phi + (dr)\,\mathbf{e}_r\\ \Leftrightarrow\quad &\mathbf{e}_t = \frac{r\dot\phi\mathbf{e}_\phi + \dot r\mathbf{e}_r}{\dot l}, \end{aligned} \tag{9}$$

where the dot represents differentiation with respect to χ. The unit normal, $\mathbf{e}_n$, may be caculated from $\mathbf{e}_t \times \mathbf{u}$. The jump conditions across γ are

$$\begin{aligned} &(\mathbf{B}^e - \mathbf{B}^i)\cdot \mathbf{e}_n = 0 \\ \Leftrightarrow \quad & r\dot{\phi}\,\partial_r(V-U) - \frac{\dot{r}}{r}(1+h^2r^2)\,\partial_\zeta(V-U) = \mu_0 i_0 hr\dot{r} \end{aligned} \tag{10}$$

and

$$\begin{aligned} &(\mathbf{B}^e - \mathbf{B}^i)\cdot \mathbf{e}_t = 0 \\ \Leftrightarrow \quad & \dot{r}\,\partial_r(V-U) + \dot{\phi}\,\partial_\zeta(V-U) = 0. \end{aligned} \tag{11}$$

The boundary collocation method forces the trial solutions of Eq. (4) to satisfy the boundary conditions, Eqs. (10) and (11), at a finite number of "collocation points" on the solenoid. When the number of collocation points is greater than the number of unknowns in U^N and V^N the matrix system may be solved by the method of least squares.

We have applied the collocation method to determine the scalar potential of a circular cross-section helical solenoid such as that shown in the $z=0$ plane in Fig. 2. The coil displacement, b, is less than its radius, a. The equation for the coil is

$$a^2 = r^2 + b^2 - 2rb\cos\zeta \tag{12}$$

which may be parametrized by ζ,

$$\dot{r} = -\frac{rb\sin\zeta}{r - b\cos\zeta}; \qquad \dot{\phi} = 1, \tag{13}$$

giving the boundary conditions

$$\frac{(a^2 + h^2r^2b^2\sin^2\zeta)}{(r - b\cos\zeta)}\,\partial_r(V-U) = -\mu_0 i_0\, hrb\sin\zeta, \tag{14}$$

and

$$\frac{(a^2 + h^2r^2b^2\sin^2\zeta)}{rb\sin\zeta}\,\partial_\zeta(V-U) = -\mu_0 i_0 hrb\sin\zeta. \tag{15}$$

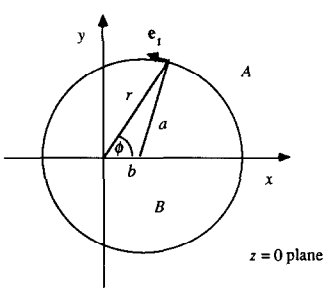

FIG. 2. A circular cross-section helical solenoid, radius a and displacement b, shown in the $z=0$ plane. Surface currents flow in the plane in the direction of $\mathbf{e}_t$.

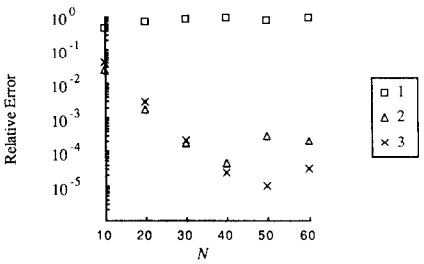

FIG. 3. Relative error versus the number of cylindrical harmonics in the expansion set for three alternative collocation schemes. Methods 1 and 2 have square matricies with the collocation points distributed in equal arcs and equal angles, respectively. Method 3 is a least squares collocation method with 90 collocation points.

Figure 3 shows the results of three collocation methods as applied to a solenoid of radius $a = 1.0$ m, displacement $b = 0.5$ m, and pitch $h = 1.0\,\mathrm{m}^{-1}$. The relative error estimate,

$$\xi^r = \frac{\mathrm{MAX}\,|U^N - V^N|}{\mathrm{MAX}\,|V^N|}, \tag{16}$$

where the maxima are chosen from those points mid-way between the collocation points, has been plotted against N. For methods 1 and 3 the collocation points were distributed in equal arcs along the contour in the $z = 0$ plane. For method 2 they were distributed in equal increments of ϕ which had the effect of concentrating them on the side of the coil closest to the z-axis. The first two methods had square matrices. The third was a least squares collocation method with 90 collocation points. The first method was inaccurate at all values of N. The other two showed an exponential decrease in ξ^r up to $N = 40$. For $N > 40$ the loss of accuracy of method 2 coincided with the matrix system becoming ill-conditioned.

The accuracy of all three collocation methods depended on the coil displacement. In contrast to Fig. 3, if $b = 0.15$ method 1 (equal arc collocation) with $N = 20$ had a

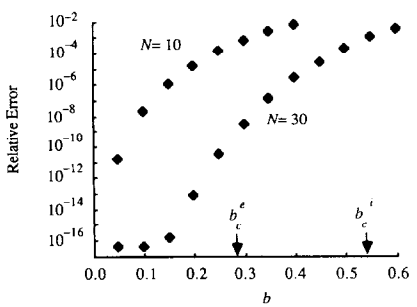

FIG. 4. Relative error of the least squares collocation method versus coil displacement for 10 and 30 cylindrical harmonics. The critical values of b for the exterior (b_c^e) and the interior (b_c^i) series are also shown.

relative error of $\xi^r = 6 \times 10^{-11}$ which was much better than equal angle collocation (method 2) ($\xi^r = 2 \times 10^{-7}$). The least squares collocation method gave the best results over a range of values of b and N and was insensitive to the placement of the collocation points. For $N = 30$, ξ^r for method 3 ranges from 10^{-16} at $b = 0.1$ to 10^{-2} at $b = 0.6$ as shown in Fig. 4. We shall return to discuss these results in Section 6.

4. Green's Theorem for the Helical Solenoid

It can be shown that [13, 14]

$$G(r, \zeta \mid r_0, \zeta_0) = -2 \ln r_> + 4 \sum_{n=1}^{\infty} I_n(nhr_<) K_n(nhr_>) \cos[n(\zeta - \zeta_0)], \tag{17}$$

where $r_> = \max(r, r_0)$ and $r_< = \min(r, r_0)$, is a helical Green's function satisfying

$$\nabla^2 G = -\frac{4\pi}{r} \delta(r - r_0)\, \delta(\zeta - \zeta_0). \tag{18}$$

Consider the integration of $U\nabla^2 G - G\nabla^2 U$ over the cut helical tube enclosed by one period, γ_p, of the helical solenoid γ of Fig. 1. Applying Green's theorem in the usual fashion we have

$$8\pi^2 h^{-1} U(r_B, \zeta_B) = \int_{\gamma_p} (G\, \partial_n U - U\, \partial_n G)\, dS \tag{19}$$

for observer points (r_B, ζ_B) inside γ_p and

$$0 = \int_{\gamma_p} (G\, \partial_n U - U\, \partial_n G)\, dS \tag{20}$$

for points (r_A, ζ_A) outside. A similar result holds for V if the integration is carried out over the volume outside of γ_p giving

$$\left.\begin{matrix} U(r_B, \zeta_B) \\ V(r_A, \zeta_A) \end{matrix}\right\} = \frac{h}{8\pi^2} \int_{\gamma_p} [G\, \partial_n (U - V) - (U - V)\, \partial_n G]\, dS. \tag{21}$$

Note the the surface integrals over the ends of the cut helical tube defined by γ_p cancel by periodicity. We can insert the boundary conditions across γ into the integral noting that the tangential condition is equivalent to $U = V + c$, where c is an arbitrary constant which we set to zero. Also, in the notation of Section 3,

$$(dS)\, \partial_n = (dz)(d\chi)[r\dot{\phi}\, \partial_r - \dot{r} r^{-1}(1 + h^2 r^2)\, \partial_\zeta]. \tag{22}$$

For a circular coil this gives (from Eqs. (10) and (13))

$$\left.\begin{matrix} U(r_B, \zeta_B) \\ V(r_A, \zeta_A) \end{matrix}\right\} = \frac{\mu_0 i_0 h}{4\pi} \int_{-\pi}^{\pi} \frac{r^2 b \sin \zeta}{r - b \cos \zeta} G\, d\zeta, \tag{23}$$

where $r(\zeta)$ is the function defined by Eq. (12). When r_A is greater than $a+b$ and when r_B is less than $a-b$, Eq. (21) returns the expansions for U and V of Eqs. (7) and (8) providing the order of the integration and summation can be interchanged. This is justified whenever the resultant series converges uniformly [15]. The coefficients a_n^i and a_n^e in Eqs. (7) are given by

$$a_n^i = \frac{i\mu_0 i_0 h}{\pi} \int_{-\pi}^{\pi} d\zeta \, r \frac{dr}{d\zeta} K_n(nhr) \exp(in\zeta), \tag{24}$$

and

$$a_n^e = \frac{i\mu_0 i_0 h}{\pi} \int_{-\pi}^{\pi} d\zeta \, r \frac{dr}{d\zeta} I_n(nhr) \exp(in\zeta). \tag{25}$$

By expanding Eqs. (24) and (25) in b/a it is possible to derive analytic approximations for the series coefficients when the coil displacement is small. For instance, to leading order the first coefficient in the interior series becomes

$$a_1^i \sim \mu_0 i_0 hab K_1(ha), \tag{26}$$

a result which has been derived by Sy by another method [16].

5. Convergence of the Cylindrical Harmonic Expansions

Because there are no sources other than the solenoid, U and V are analytic everywhere throughout their domains of definition (B and A, respectively, including γ if it is smooth). The Fourier–Bessel series of Eqs. (7) and (8) also define analytic functions throughout those parts of the interior and exterior regions where they converge. In the previous section we showed the equivalence of these series to the Green's function integral expression for U (and V) inside (and outside) the inner (and outer) cylinder tangential to γ. The series must continue to be valid representations of the potentials throughout the intersection of their domains of definition and their regions of convergence. In this section we determine these regions by considering the large-n asymptotic behaviour of the a_n's using the technique of saddle point integration in the complex plane.

It will be convenient to change the variable of integration in Eqs. (24) and (25) from ζ to $u \equiv r^2$. The definite integral in terms of ζ can be shown to be equivalent to an integration about a closed contour in the complex u plane as follows. The inverse function, $\zeta(u)$ of Eq. (12), can be written

$$\begin{aligned} \zeta(u) &= \arccos\left(\frac{u+b^2-a^2}{2bu^{1/2}}\right) \equiv \arccos w \\ &= -i \ln[w \pm (w^2-1)^{1/2}]. \end{aligned} \tag{27}$$

The argument of the logarithm has branch points at $w = \pm 1$ or at $u = (a-b)^2$ and $u = (a+b)^2$. We take the branch cut to join these points along the real axis. In the u plane there is an additional cut along the negative real axis to keep $u^{1/2}$ single valued, as in Fig. 5a. For $w = x + i\varepsilon$ with $|x| \leqslant 1$ it can be seen that

$$\zeta \sim \arg[x \pm \operatorname{sign}(\varepsilon)\, i(1-x^2)^{1/2}] \tag{28}$$

to leading order in ε. Thus, the value of $\zeta \in (-\pi, \pi)$ around the circumference of the coil will be returned by shrinking a clockwise contour of

$$\zeta(u) = -i \ln\left(\frac{u + b^2 - a^2 - [u-(a+b)^2]^{1/2}[u-(a-b^2]^{1/2}}{2bu^{1/2}}\right) \tag{29}$$

onto the isolated cut in the u (or w) plane. This corresponds to the choice of the minus sign in Eqs. (27) and (28). Note that when we change the variable of integration to u the functional dependence of the integrand on ζ is via $\exp(in\zeta)$ only, so that there is no additional cut due to the logarithm. Note also that the range of $\exp(in\zeta)$ is the *interior* of the unit circle.

The integrals of Eqs. (24) and (25) now become

$$a_n^e = \frac{i\mu_0 i_0 h}{2\pi} \int_C du\, \mathscr{C}_n^{(+)}(nhu^{1/2}) \exp[in\zeta(u)] \tag{30}$$

and

$$a_n^i = \frac{i\mu_0 i_0 h}{2} \int_C du\, \mathscr{C}_n^{(-)}(nhu^{1/2}) \exp[in\zeta(u)], \tag{31}$$

where the contour C is as shown in Fig. 5a. For brevity in the following analysis we have defined the functions

$$\mathscr{C}_n^{(+)}(\bullet) \equiv I_n(\bullet), \qquad \mathscr{C}_n^{(-)}(\bullet) \equiv \frac{1}{\pi} K_n(\bullet). \tag{32}$$

To find the large-n behaviour of the a_n's we seek to deform C to pass through a saddle point in the absolute value of the integrand along the line of steepest descent

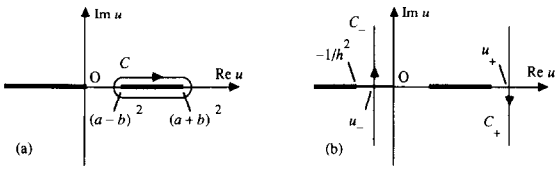

FIG. 5. (a) The complex u plane showing the cuts needed to make $\exp[i\zeta(u)]$ single valued, and the contour C in Eqs. (30) and (31). (b) The deformed contours C_+ and C_- crossing the saddle points u_+ and u_-.

[17]. We use the large order, large argument asymptotic forms [18] for I_n and K_n, summarized by

$$\mathscr{C}_n^{(\sigma)}(nhu^{1/2}) \sim \frac{\exp[\sigma n\eta(u)]}{(2\pi n)^{1/2}(1+h^2u)^{1/4}} \tag{33}$$

for $n \to \infty$, where

$$\eta(u) \equiv (1+h^2u)^{1/2} + \ln\left(\frac{hu^{1/2}}{1+(1+h^2u)^{1/2}}\right), \tag{34}$$

and $\sigma = +$ corresponds to the exterior (e) expansion and $\sigma = -$ corresponds to the interior (i) expansion.

Equations (30) and (31) can both be written in terms of the integral

$$\mathscr{I}_n^{(\sigma)} \equiv \frac{h^2}{2}\int_C du\, \mathscr{C}_n^{(\sigma)}(nhu^{1/2}) \exp[in\zeta(u)]. \tag{35}$$

Substituting Eq. (33) into Eq. (35) we find

$$\mathscr{I}_n^{(\sigma)} \sim \frac{h^2}{2(2\pi n)^{1/2}}\int_C du \frac{\exp[-nf_\sigma(u)]}{(1+h^2u)^{1/4}}, \tag{36}$$

where

$$f_\sigma(u) \equiv i\zeta(u) + \sigma\eta(u). \tag{37}$$

The saddle points are obtained by finding the stationary points of $f_\sigma(u)$. That is, they are the roots of the equation

$$f'_\sigma(u) = 0. \tag{38}$$

After substituting Eqs. (29) and (34) into Eq. (37), writing Eq. (38) in the form $i\zeta'(u) = -\sigma\eta'(u)$, and squaring we find a quadratic equation whose roots are

$$u_\pm \equiv a^2 + b^2 \pm 2\mu ab, \tag{39}$$

where

$$\mu \equiv (1+b^{-2}h^{-2})^{1/2}. \tag{40}$$

Because of the squaring operation, one or both of $u_\pm$ may be spurious as roots of Eq. (38). We must distinguish two cases:

Case I. $h^2 > (a^2-b^2)^{-1}$, $u_- > -1/h^2 > b^2 - a^2$, $\mu < a/b$. In this case the only zero of $f'_+(u)$ is u_+, and the only zero of $f'_-(u)$ is u_-. Evaluating $f(u)$ and $f''(u)$ at these saddle points we find

$$f_+(u_+) = h(a+\mu b) + \ln\left(\mu - \frac{1}{hb}\right), \tag{41}$$

$$f''_+(u_+)=\frac{\mu b h^3}{4a(a+\mu b)}, \tag{42}$$

$$f_-(u_-\pm i0)=\mp i\pi - h(a-\mu b)+\ln\left(\mu-\frac{1}{hb}\right), \tag{43}$$

$$f''_-(u_-)=\frac{\mu b h^3}{4a(a-\mu b)}. \tag{44}$$

Note that $\exp f_-(u)$ is continuous in the neighbourhood of u_- because the jump in $f_-(u)$ is $2\pi i$.

Case II. $h^2<(a^2-b^2)^{-1}$, $-1/h^2<u_-<b^2-a^2<0$, $\mu>a/b$. In this case *both* u_+ *and* u_- are zeros of $f_+(u)$, whereas $f_-(u)$ has *no* zeros (on the principal sheet defined by Eq. (29)). Equations (41) and (42) remain valid, while

$$f_+(u_-)=h(\mu b-a)+\ln\left(\mu-\frac{1}{hb}\right), \tag{45}$$

$$f''_+(u_-)=\frac{\mu b h^3}{4a(a-\mu b)}. \tag{46}$$

Except in the case $h^2<(a^2-b^2)^{-1}$, $\sigma=-$, it is topologically possible to deform C to cross the highest saddle point along the path of steepest descent and so find the leading order, large-n asymptotic behaviour of $\mathscr{I}_n^\sigma$. For instance, in the case $h^2<(a^2-b^2)^{-1}$, $\sigma=+$, there are two saddle points, but it is the one at $u=u_+$ which is relevant because $f_+(u_+)=f_+(u_-)+2ha>f_+(u_-)$, and C can be deformed to the contour C_+ in Fig. 5b, as is also the case for $h^2>(a^2-b^2)^{-1}$, $\sigma=+$. In the case $h^2>(a^2-b^2)^{-1}$, $\sigma=-$, the contour C_- of Fig. 5b is to be used. This is true even if u_- is negative since inspection of Eqs. (29), (34), and (37) shows that the $\ln u^{1/2}$ terms in $i\zeta(u)$ and $\eta(u)$ either cancel or combine to give $-\ln u$ in $f_\sigma(u)$, so the cut along the negative real axis can be ignored for the integrand of Eq. (36). (One can also show that $\zeta(u)\to 0$ as $u\to 0$ sufficiently fast that there is never a pole at the origin.) Expanding the integrals about the saddle points and integrating we find the leading order, large-n asymptotic behaviour in the expansion coefficients to be

$$a^e\sim\frac{\mu_0 i_0}{n\pi h}\left(\frac{a}{\mu b}\right)^{1/2}\exp(nc_+), \tag{47}$$

and

$$a^i\sim\frac{(-)^{n+1}\mu_0 i_0}{nh}\left(\frac{a}{\mu b}\right)^{1/2}\exp(nc_-), \tag{48}$$

where μ is given by Eq. (40) and

$$c_\sigma\equiv\sigma h(a+\sigma\mu b)+\ln(\mu-h^{-1}b^{-1}). \tag{49}$$

Although Eq. (48) has been derived assuming Case I, $\mu < a/b$, it can be shown to be valid even in Case II (as might be expected from analytic continuation since there is no singularity when $a = \mu b$). This is shown by deforming C to wrap around the negative real axis and evaluating the contribution of the cut. In this way we can show that

$$\mathscr{I}_n^{(-)} = \frac{-i(-)^n h^2}{2} \int_{-\infty - i0}^{-i0} du\, I_n(nhu^{1/2}) \exp[in\zeta(u)]. \tag{50}$$

One may verify from Debye's formula [19] that Eq. (33) remains valid as the leading order behaviour of $I_n(nhu^{1/2})$ on the cut, provided $u > -1/h^2$. Thus the subdominant saddle point for $\mathscr{I}_n^{(+)}$, u_-, becomes the relevant saddle point for $\mathscr{I}_n^{(-)}$ and Eq. (48) again results.

To determine the radii of convergence of the series of Eqs. (7) and (8) we need to use both the asymptotic behaviour of the expansion coefficients, Eqs. (47) and (48), *and* that of the Bessel functions, Eq. (33). The radius of convergence, r_c, corresponds to the cylinder on which the exponential divergence of one is just balanced by the exponential convergence of the other. For the exterior and interior problems it is found by solving the transcendental equations

$$\eta(r_c^e) = c_+, \tag{51}$$

or

$$\eta(r_c^i) = -c_-, \tag{52}$$

where η is given by Eq. (34) and $c_\pm$ by Eq. (49). The exterior expansion converges absolutely for $r > r_c^e$, and the interior expansion converges absolutely for $r = r_c^i$.

Some representative values of r_c^σ are given in Table I. We have checked some of these results numerically by estimating the limiting ratio of the terms in the interior and exterior series as calculated by the Green's function method. The fact that

TABLE I

Examples of Radii of Convergence Calculated from Eqs. (51) and (52) for the Exterior (r_c^e) and Interior (r_c^i) Series

h	a	b	r_c^e	r_c^i
0.8	1.0	0.5	1.00	2.08
1.0	1.0	0.25	0.63	2.28
1.0	1.0	0.3	0.73	2.11
1.0	1.0	0.5	1.10	1.62
1.0	1.0	0.7	1.41	1.30
2.0	1.0	0.5	1.36	0.87
∞	a	b	$a+b$	$a-b$

$r_c^e < a+b$ for finite h means that, as far as the exterior field is concerned, the solenoid could be replaced by an equivalent helical sheet current flowing on the surface of a cylinder of radius r_c^e, interior to the radius of the outermost point of the solenoid [20]. Similarly, the interior field could be reproduced by a helical sheet current on a cylinder of radius r_c^i, greater than the radius of the innermost point of the solenoid.

If $r_c^e < a-b$, the exterior harmonic expansion converges throughout A, and if $r_c^i > a+b$ the interior harmonic expansion converges throughout B. It turns out that $r_c^e < a-b$ in the case $a=h=1$ while b is less than a critical value $b_c^e \approx 0.2888$ whereas $r_c^i > a+b$ while b is less than a critical value $b_c^i \approx 0.5441$. Thus the convergence criterion is not as stringent for the interior expansion, which is fortunate because this is often the case of physical interest (since we often need an accurate and efficient representation of the magnetic field in the vicinity of a plasma confined to the interior region).

6. Discussion

Figure 4 shows the dependence of the relative error of the least squares collocation method on the coil displacement, b, for two values of N in the case $a=h=1$. The critical values b_c^e and b_c^i are also shown. It is seen that the error appears to be a smooth function of b well beyond the point where convergence of the infinite series for the exterior part of the solution ceases. The situation is different for the square matrix, equal arc collocation method which, as we saw in Section 3, becomes very inaccurate at moderate coil displacements—presumably because not enough collocation points are placed on the inside of the coil where the exterior series should diverge. We can also see from Fig. 3 that in the case $b=0.5>b_c^e$ there appears to be exponential convergence of the least squares and equal angle collocation methods with respect to N up to $N \approx 40$ which is where matrix ill-conditioning sets in. If we assume that the ill-conditioning is a result of the finite precision of the computation then we have the seemingly paradoxical result that some boundary collocation methods would appear capable of giving arbitrary precision beyond the region of convergence of an infinite series in the same set of basis functions.

Thus our results indicate that, for example, Brazier-Smith [8] was overly pessimistic about the dangers of harmonic expansion, provided enough expansion functions and the more robust least squares collocation method are used. The resolution of the paradox is presumably that the expansion sets remain *complete* beyond their radii of convergence. Rather than prove this we give a simple analogy. Consider the function

$$f(x)=(1+x)^{-1} \tag{53}$$

on the interval $[0, 2]$. We know that $\{x^n \mid n=0, 1, 2, \ldots\}$ forms a complete expan-

sion set for $f(x)$ from the Weierstrass approximation theorem [21]. For example, the sequence of partial sums

$$f_n(x) = \frac{1}{2} \sum_{m=0}^{n} \left(\frac{1-x}{2}\right)^m = \sum_{m=0}^{n} a_m^n x^m, \tag{54}$$

where

$$a_m^n \equiv \frac{(-1)^m}{2} \sum_{l=m}^{n} \left(\frac{1}{2}\right)^l \binom{l}{m}, \tag{55}$$

converges to $f(x)$ as $n \to \infty$ for x in the given interval. Yet the series

$$\sum_{m=0}^{\infty} (-1)^m x^m \tag{56}$$

does not converge to $f(x)$ beyond $x = 1$. Thus completeness and series convergence are two quite distinct questions.

Since the series of Eq. (56) converges to $f(x)$ over the subinterval $[0, 1)$, we must have $a_m^n \to (-1)^m$ as $n \to \infty$ with m fixed. However we also see from Eq. (55) that $a_n^n = (-1)^n/2^{n+1} \to 0$ as $n \to \infty$. Thus the superior convergence of the sequence $f_n(x)$ is achieved by smoothly reducing the a_n^n in absolute magnitude as $m \to n$ relative to the $(-1)^m$ coefficients found from the partial sums of the series of Eq. (56). We see from Fig. 6 that the least squares collocation method does a similar thing to the expansion coefficients for the harmonic expansion.

The convergence of the sum $\sum_m a_m^n x^m$ toward $f(x)$ in the region outside the radius of convergence of Eq. (56) must depend on cancellation of the low-m contributions in the sum by the $m = O(n)$ contributions, since the a_m^n approximate the coefficients of the divergent series when $m \ll n$. This cancellation effect means that all terms of the partial sum are important and that, as a practical method, harmonic representations will rapidly become uneconomical if pushed too far beyond the radius of convergence. It also helps explain why convergence ceases when the number of terms becomes large—rounding errors will become very important.

Finally, Figs. 7a and b show the contours of the scalar potential and the helical

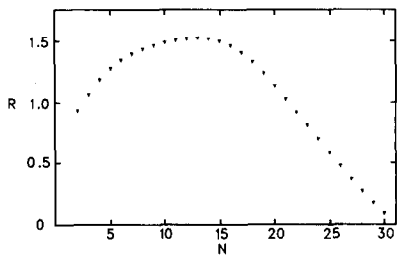

FIG. 6. Ratios, R, of the magnitudes of consecutive terms in the exterior series for a helical solenoid of circular cross section, $a = h = 1$, $b = 0.5$. The ratios $R = |a_n^e K_n(nhr)|/|a_{n-1}^e K_n[(n-1)hr]|$ are evaluated at $r = 0.5$. The series was calculated using least squares collocation with 90 collocation points and 30 expansion functions.

flux of the helical solenoid of the SHEILA heliac [22]. Although these results were obtained using least squares collocation, it was found that the radius of convergence of the interior series included the entire interior region so that it was possible to use a series calculated from the Green's function integral in free-boundary equilibrium calculations [6]. Our establishment of *a priori* convergence criteria helps make the Green's function-harmonic expansion method an attractive alternative to collocation. If collocation is to be used the maximum errors on the boundary should be calculated and compared with an exact technique (such as using the Bio–Savart integral of the current distribution).

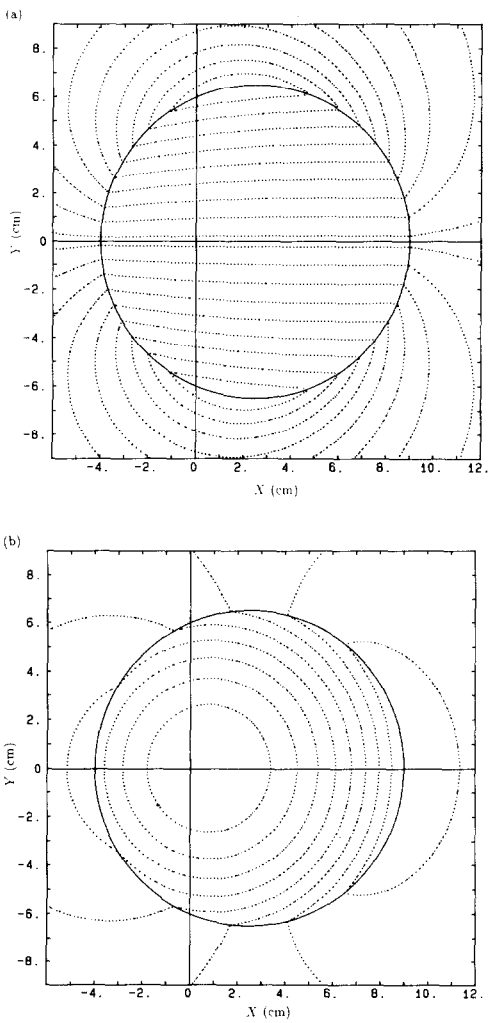

FIG. 7. (a) Scalar potential for the solenoid of the helically symmetric limit of the SHEILA heliac in the $z = 0$ plane ($a = 0.065$ m, $b = 0.025$ m, $h = 16.0\ \text{m}^{-1}$). Least squares collocation was used with 90 collocation points and 30 expansion functions. (b) Helical flux for the solenoid of Fig. 7(a).

ACKNOWLEDGMENTS

We wish to acknowledge useful discussions with Dr. A. D. Miller, Dr. R. G. Storer, and Dr. W. N-C. Sy.

REFERENCES

1. A. H. BOOZER, T. K. CHU, R. L. DEWAR, H. P. FURTH, J. M. GREENE, J. L. JOHNSON, R. M. KULSRUD, D. A. MONTICELLO, G. KUO-PETRAVIC, G. V. SHEFFIELD, S. YOSHIKAWA, AND O. BETANCOURT, *Plasma Physics and Controlled Nuclear Fusion Research*, Vol. 3, p. 129 (Int. At. Energy Assoc., Vienna, 1983).
2. S. YOSHIKAWA, *Nucl. Fusion* **23**, 667 (1983).
3. J. H. HARRIS, J. L. CANTRELL, T. C. HENDER, B. A. CARRERAS, AND R. N. MORRIS, *Nucl. Fusion* **25**, 623 (1985).
4. R. L. DEWAR, D. A. MONTICELLO, AND W. N-C. SY, *Phys. Fluids* **26**, 1723 (1984).
5. H. P. FURTH, J. KILLEEN, M. N. ROSENBLUTH, AND B. COPPI, *Plasma Physics and Controlled Nuclear Fusion Research*, Vol. 1 p. 103 (Int. At. Energy Assoc., 1966).
6. H. J. GARDNER, R. L. DEWAR, AND W. N-C. SY, *J. Comput. Phys.* **74**, 477 (1988).
7. J. DELUCIA, S. C. JARDIN, AND A. M. TODD, *J. Comput. Phys.* **37**, 183 (1980).
8. P. R. BRAZIER-SMITH, *J. Comput. Phys.* **54**, 524 (1984).
9. R. L. DEWAR AND H. J. GARDNER, Australian National University (Research School of Physical Sciences) Report No. ANU/TPP86/03, 1987 (unpublished).
10. J. D. JACKSON, *Classical Electrodynamics* (Wiley, New York, 1962).
11. R. COURANT AND D. HILBERT, *Methods of Mathematical Physics*, Vol. 2 (Interscience, New York, 1962).
12. B. A. FINLAYSON, *The Method of Weighted Residuals and Variational Principles* (Academic Press, New York, 1972).
13. H. J. GARDNER, Ph.D. thesis, Australian National University, 1986.
14. P. MERKEL, *Z. Naturf.* **37a**, 859 (1982).
15. E. T. WHITTAKER AND G. N. WATSON, *A Course of Modern Analysis*, p. 78 (Cambridge Univ. Press, London, 1965).
16. W. N-C. SY private communication.
17. G. N. WATSON, *A Treatise on the Theory of Bessel Functions*, p. 235 (Cambridge Univ. Press, London, 1966).
18. M. ABRAMOWITZ AND I. A. STEGUN, *Handbook of Mathematical Functions*, p. 378 (Dover, New York, 1972).
19. M. ABRAMOWITZ AND I. A. STEGUN, *Handbook of Mathematical Functions*, p. 366 (Dover, New York, 1972).
20. J. M. GREENE, *Phys. Fluids* **8**, 704 (1965).
21. G. DAHLQUIST AND A BJÖRK, *Numerical Methods*, translated by N. Anderson (Prentice–Hall, Englewood Cliffs, NJ, 1974).
22. B. D. BLACKWELL, S. M. HAMBERGER, L. E. SHARP, AND X. H. SHI, *Nucl. Fusion* **25**, 1485 (1985).